Improved Impedance-Pattern Generation for Automatic Noise-Parameter Determination

Sven Van den Bosch, *Member, IEEE,* and Luc Martens, *Member, IEEE*

***Abstract*—The correlation between the impedance pattern for automatic noise-parameter determination and the accuracy of extracted parameters is investigated using a statistical approach. Selection criteria for near-optimal patterns are given, and a new method is proposed for automatic generation of these patterns. Simulations prove this method outperforms others using random or cross-shaped patterns.**

***Index Terms*—Impedance, noise, noise measurement.**

I. Introduction

DURING the last decade, the tendency toward smaller device geometries and lower bias supply voltages has given increasing importance to measurement and modeling of device noise behavior. For measurements, the multi-impedance technique originally proposed by Lane [1] is generally accepted. State-of-the-art setups use electronic or mechanical impedance tuning to generate impedance patterns for the measurement. It has been pointed out that the selected pattern strongly influences the accuracy with which noise parameters can be extracted [2], [3]. Davidson *et al.* [2] investigated a cross-shaped pattern and concluded that accurate noise-parameter extraction only required the source impedances to be "well spread" over the Smith chart. The proximity to $\Gamma_{\rm opt}$ was not a factor according to them. Sannino [3] identified *singular loci* on the Smith chart. Impedance patterns comprising impedances that are on one singular locus give rise to matrix singularities in the extraction procedure. Therefore, source impedances on two or more singular loci are to be chosen. However, no real effort was undertaken to find an algorithm to generate a near-optimal pattern. We will show that the existing practice is far from near-optimal, and propose a new algorithm suitable for automatic measurements.

A number of techniques have been proposed for noise-parameter extraction [4]–[6]. The method used by Boudiaf [6] was reported to be the most accurate [7]. For simplicity and because of its familiarity, we used the extraction technique originally proposed by Lane in this paper. In Section II, we will briefly summarize the existing practice in noise-parameter extraction. Section III derives selection criteria for near-optimal impedance patterns. Section IV compares simulations with randomly distributed and cross-shaped patterns to a newly developed two-step-pattern generation technique. This technique is proved to be superior to the existing ones. Section V sums up the most important results and conclusions.

Manuscript received October 20, 1997; revised April 1, 1998. The work of S. Van den Bosch was supported by the Vlaams Instituut voor de Bevordering van het Wetenschappelijk-Technologisch onderzoek in de industrie.

The authors are with the Department of Information Technology, University of Gent, 9000 Gent, Belgium (e-mail: vdbosch@intec.rug.ac.be).

Publisher Item Identifier S 0018-9480(98)08028-4.

II. State-of-the-Art Impedance Patterns

The noise figure depends nonlinearly on the source impedance as described by

$$F(\Gamma_s) = F_{\rm min} + \frac{4 \cdot R_n}{Z_0} \cdot \frac{|\Gamma_s - \Gamma_{\rm opt}|^2}{(1-|\Gamma_s|^2)\cdot|1+\Gamma_{\rm opt}|^2}. \quad (1)$$

In (1), Γ_s is the reflection coefficient of the source impedance, $\Gamma_{\rm opt}$ is the optimum source impedance (yielding minimum noise figure $F_{\rm min}$), and R_n is a measure of the gradient with which the noise figure increases for impedance points further away from $\Gamma_{\rm opt}$.

Lane [1] developed a method to solve (1) for $F_{\rm min}$, R_n, and $\Gamma_{\rm opt}$ from a set of measurements at different source impedances by a least-squares fit. The key step in this method is the solution of a linear set of the four equations in four unknowns $B = A \cdot X$, shown in (2), at the bottom of the following page.

Possible singularities in A depend solely on the choice of the source admittances $Y_{si} = G_{si} + j \cdot B_{si}$. Specific patterns called *singular loci* give rise to these singularities [3]. Closed-form expressions for these singular loci are given in

$$G_s = c \quad B_s = c \quad |Y_s|^2 = c$$
$$|Y_s|^2/G_s = c \quad |Y_s|^2/B_s = c$$
$$|Y_s|^2/G_s = c + c'/G_s \quad (c \text{ and } c' \text{ are constants}). \quad (3)$$

A special case of the last equation in (3) is

$$|Y_s|^2/G_s = c - 1/G_s. \quad (4)$$

This represents circles in the G_s–B_s-plane and concentric circles around the origin on a Smith chart. Sannino proposes to use source admittances on two or more different singular loci to avoid singularity [3]. The cross-shaped pattern investigated by Davidson *et al.* is a special case of this since it consists of admittances located on three different singular loci (see Fig. 1).

III. Selection Criterion for the Optimum Admittance Pattern

A. Condition Number

Since the key step in Lane's method is the solution of the linear set of equations $B = A \cdot X$ [shown in (2)], a logical candidate for selecting an optimum pattern is the condition

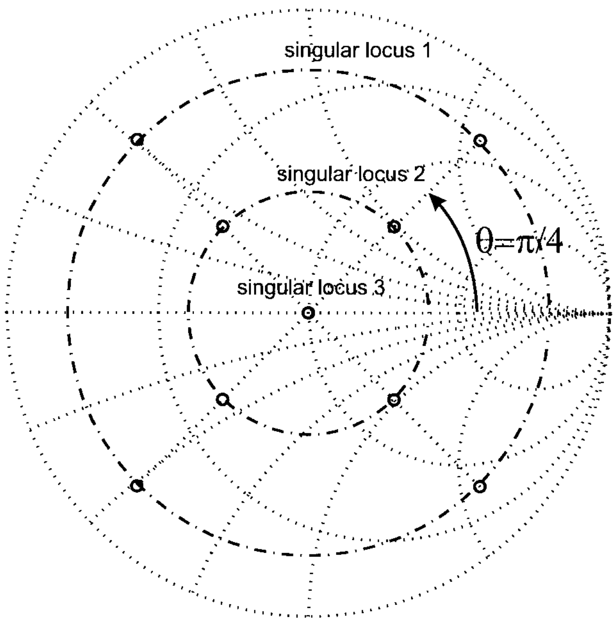

Fig. 1. Cross-shaped pattern consisting of three different singular loci.

number of A. The condition number of a matrix A indicates the stability of the solution X of $B = A \cdot X$ with respect to errors in B. Since A is completely determined by the selected admittances, its condition number depends only on the admittance pattern. We investigated the possibility of using the condition number of A by generating a large number (500) of random admittance patterns with a maximum reflection coefficient $\Gamma_{\max} = 0.9$. For each pattern, noise figures were calculated using (1) with parameter values $F_{\min} = 2.15$ dB, $R_n = 120\ \Omega$, and $Y_{\rm opt} = 0.25 - j0.5$. The resulting noise figures were then given a random distributed error with a 1%, 2%, and 5% maximum error, respectively. These were regarded as measured noise figures. For each admittance pattern, the four noise parameters and the matrix condition number were then calculated. Finally, correlation coefficients between noise-parameter errors (with respect to the exact values) and the matrix condition number were then calculated. For the condition number to be a valid selection criterion, a large correlation coefficient (close to one) is expected. Correlation coefficients between all four parameters ($F_{\min}$, R_n, $G_{\rm opt}$, and $B_{\rm opt}$) and the condition number for a maximum 5% error are shown in Table I. In Table I, *RC* denotes the inverse of the condition number.

TABLE I
CORRELATION BETWEEN CONDITION NUMBER AND NOISE-PARAMETER ERRORS FOR A MAXIMUM 5% ERROR ON NOISE FIGURES

	RC	F_{min}	R_n	G_{opt}	B_{opt}
RC	1	0.1265	0.3602	-0.0138	0.1686
F_{min}		1	0.1951	0.6507	0.8022
R_n			1	0.0273	0.3484
G_{opt}				1	0.5997
B_{opt}					1

Table I shows that the error on none of the noise parameters is correlated with the matrix condition number. Therefore, the condition number is not a good criterion for selecting the optimum pattern.

B. Confidence Interval of Statistic Distribution

Since the condition number is not a good criterion for selecting the admittance pattern, we adopt a statistical approach. The procedure is as follows. We start from a set of noise parameters

$$B = \begin{bmatrix} \sum_{i=1}^{n} F_i \\ \sum_{i=1}^{n} F_i \cdot \left(G_{si} + \dfrac{B_{si}^2}{G_{si}}\right) \\ \sum_{i=1}^{n} F_i \sum_{i=1}^{n} \left(\dfrac{1}{G_{si}}\right) \\ \sum_{i=1}^{n} F_i \sum_{i=1}^{n} \left(\dfrac{B_{si}}{G_{si}}\right) \end{bmatrix}$$

$$X = \begin{bmatrix} F_{\rm min} - 2 \cdot R_n \cdot G_{\rm opt} \\ R_n \\ R_n \cdot \left(G_{\rm opt}^2 + B_{\rm opt}^2\right) \\ -2 \cdot R_n \cdot B_{\rm opt} \end{bmatrix}$$

$$A = \begin{bmatrix} n & & & (a_{jk} = a_{kj}) \\ \sum_{i=1}^{n} \left(G_{si} + \dfrac{B_{si}^2}{G_{si}}\right) & \sum_{i=1}^{n} \left(G_{si} + \dfrac{B_{si}^2}{G_{si}}\right)^2 & & \\ \sum_{i=1}^{n} \left(\dfrac{1}{G_{si}}\right) & \sum_{i=1}^{n} \left(1 + \dfrac{B_{si}^2}{G_{si}^2}\right) & \sum_{i=1}^{n} \left(\dfrac{1}{G_{si}^2}\right) & \\ \sum_{i=1}^{n} \left(\dfrac{B_{si}}{G_{si}}\right) & \sum_{i=1}^{n} \left(B_{si} + \dfrac{B_{si}^3}{G_{si}^2}\right) & \sum_{i=1}^{n} \left(\dfrac{B_{si}}{G_{si}^2}\right) & \sum_{i=1}^{n} \left(\dfrac{B_{si}}{G_{si}}\right)^2 \end{bmatrix} \tag{2}$$

($F_{\min} = 2.15$ dB, $R_n = 120\ \Omega$, and $Y_{\rm opt} = 0.25 - j0.5$) and simulate the corresponding noise figures using (1). We then add a randomly distributed "error" with a fixed maximum (e.g., 5%) to each of these N sets of "synthetic measurements." For each set, the noise parameters are then calculated. We thus obtain a statistical distribution for each parameter with mean μ and standard deviation σ. In the event that the distribution is normal, the standard deviation corresponds to a 68% *confidence interval*, which means that 68% of the results are in the interval $[\mu - \sigma, \mu + \sigma]$. For nonnormal distributions, this is not exactly true, but if the distribution is not too far from normal, the conclusions drawn from the normal case can still be used and, in fact, it is common practice in statistics to do so. If N is chosen sufficiently large (we take $N = 1000$), a narrower confidence interval indicates a smaller influence of measurement errors on parameter extraction. Using this method, we will investigate the characteristics of random and cross-shaped patterns and propose a new two-step pattern that is suitable for automatic measurements and outperforms both of the other patterns.

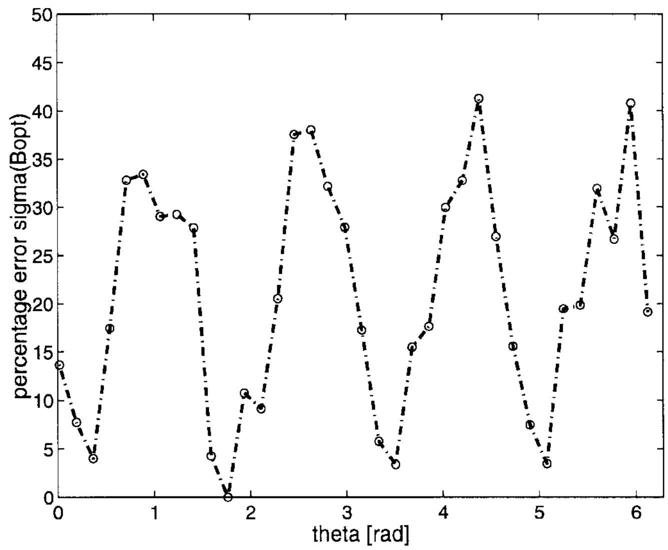

Fig. 2. Percentage error on the standard deviation of $B_{\rm opt}$ with respect to the minimal standard deviation for a cross-shaped pattern as a function of the orientation angle θ.

IV. Simulations

A. Random Pattern

For reference purposes and to get an idea of what a near-optimal pattern would look like, a large number (500) of random impedance patterns were treated as explained above. The results are again presented for $F_{\min} = 2.15$ dB, $R_n = 120\ \Omega$, and $Y_{\rm opt} = 0.25 - j0.5$, but they were calculated for a number of different combinations, and they remain valid for a wide range of noise parameters, as will become clear in Section IV-C. The following qualitative conclusions were drawn from visual inspection of the simulated patterns.

1) In most cases, the optimum pattern is different for each parameter. There is no general optimum pattern.
2) Contrary to the conclusions given by Davidson *et al.* [2], the confidence interval does depend on the proximity of measured points to $\Gamma_{\rm opt}$. $\sigma_{F_{\min}}$ especially appears to be strongly dependent on this. An explanation for the different results could be that Davidson's conclusions were drawn from the difference between the mean of the statistical distribution and the original parameter. This is not a relevant comparison since it does not indicate how far the measured noise parameters can actually be off from the real ones.
3) σ_{R_n} depends least on the selected admittance pattern, and is determined mainly by the spread of the admittances some distance away from $\Gamma_{\rm opt}$.
4) $\sigma_{G_{\rm opt}}$ and $\sigma_{B_{\rm opt}}$ are determined mainly by the number of impedances with real and imaginary part greater than that of $\Gamma_{\rm opt}$.

These qualitative conclusions were then verified quantitatively by calculating (5)–(7), shown at the bottom of this page.

For (5) and (6), the exponent in the summation is always positive when $|\mathrm{real}(\Gamma_s^i)| \geq |\mathrm{real}(\mu_{\Gamma_{\rm opt}})|$ or $|\mathrm{imag}(\Gamma_s^i)| \geq |\mathrm{imag}(\mu_{\Gamma_{\rm opt}})|$, respectively. This indicates that the number of points between $\Gamma_{\rm opt}$ and the border of the Smith chart is inversely correlated to the standard deviation on $G_{\rm opt}$ and $B_{\rm opt}$, respectively. Similarly, (7) indicates that $\sigma_{F_{\min}}$ is directly correlated $|\Gamma_s^i - \mu_{\Gamma_{\rm opt}}|$ or, in other words, with the proximity of Γ_s^i to $\Gamma_{\rm opt}$. We will use these results together with the qualitative conclusion for R_n to propose a new pattern in Section IV-C.

For comparison with the cross-shaped pattern and the two-step pattern, additional simulations were carried out to study the influence of the noise parameters (or, in fact, the influence of the device-under-test) on the extraction accuracy. Therefore, we simulated results for random patterns with $F_{\min} = 0.25$ to 8 dB in steps of 0.25 dB, $R_n = 10$ to 120 Ω in steps of 10 Ω, and for 500 different locations of $\Gamma_{\rm opt}$ distributed

$$\mathrm{corr}\left(\sum_i \exp\big(\big(\mathrm{sgn}\big(\mathrm{real}\big(\mu_{\Gamma_{\rm opt}}\big)\big)\big)\big(\mathrm{real}\big(\Gamma_s^i\big) - \mathrm{real}\big(\mu_{\Gamma_{\rm opt}}\big)\big)\big), \sigma_{G_{\rm opt}}\right) = -0.602 \tag{5}$$

$$\mathrm{corr}\left(\sum_i \exp\big(\big(\mathrm{sgn}\big(\mathrm{imag}\big(\mu_{\Gamma_{\rm opt}}\big)\big)\big)\big(\mathrm{imag}\big(\Gamma_s^i\big) - \mathrm{imag}\big(\mu_{\Gamma_{\rm opt}}\big)\big)\big), \sigma_{B_{\rm opt}}\right) = -0.660 \tag{6}$$

$$\mathrm{corr}\left(\sum_i \exp\big(-\big|\Gamma_s^i - \mu_{\Gamma_{\rm opt}}\big|^2\big), \sigma_{F_{\min}}\right) = -0.598 \tag{7}$$

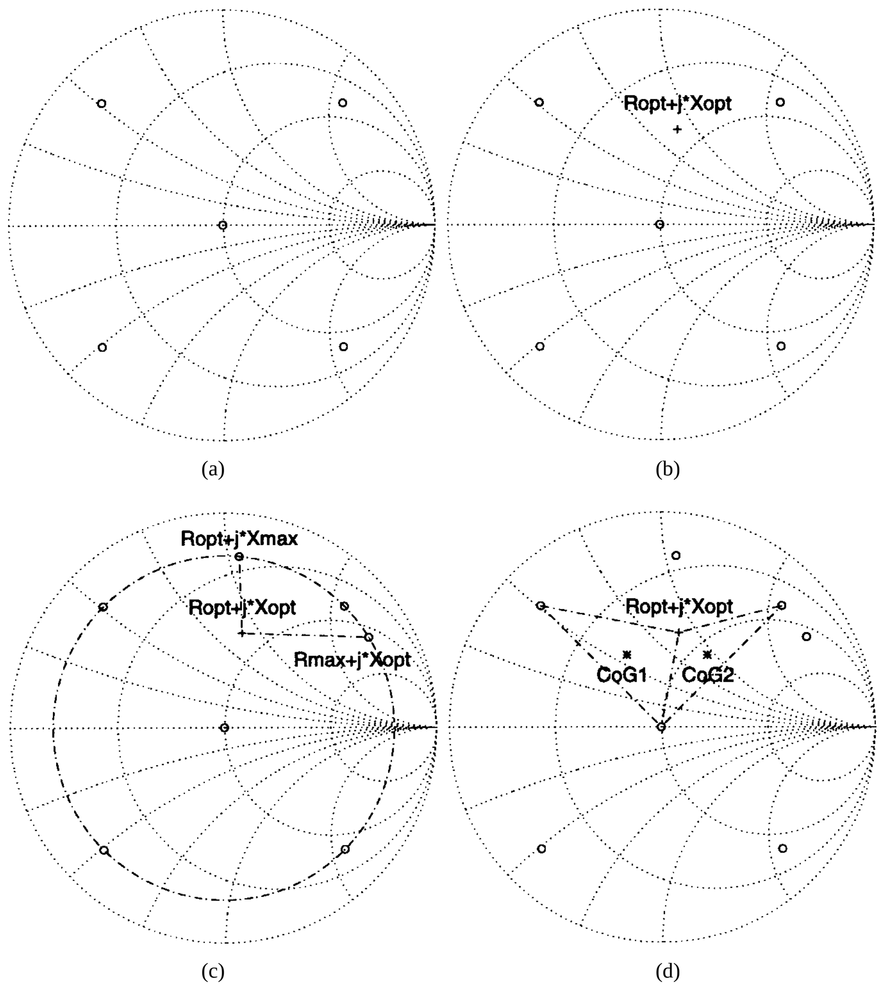

Fig. 3. Selection of additional points for two-step method.

randomly over the Smith chart. The results are compared in Section IV-C.

B. Cross-Shaped Pattern

The same simulations were performed with a cross-shaped pattern, for comparison with the results obtained by Davidson *et al.* [2]. In addition, the dependence of the accuracy on the orientation angle θ of the cross-shape was investigated. Percentage differences for all $\sigma_{B_{\rm opt}}$ with respect to the smallest $\sigma_{B_{\rm opt}}$ (for $\theta = 5 \cdot \pi/3$ rad) are given in Fig. 2, which indicates that the orientation dependence cannot be neglected.

C. New Two-Step Pattern

Based on our qualitative and quantitative conclusions discussed in Section IV-A, we present a new pattern that can be generated automatically for all measurements, but still takes into account the accuracy issues discussed earlier. We propose to use a two-step generation process. For illustration, we will use a typical nine-point impedance pattern, which is generally accepted as a good compromise between accuracy and measurement speed. Fig. 3 clarifies the pattern-selection algorithm described below. In the first step, five fixed points are measured in a cross-shaped pattern [see Fig. 3(a)] with a maximum reflection coefficient determined by the measurement setup (cables and tuner). From these points, estimates for all four noise parameters are obtained using Lane's method. $\Gamma_{\rm opt}$ obtained in this manner [see Fig. 3(b)] is then used for selecting four additional points. The first two of these address the accuracy of $G_{\rm opt}$ and $B_{\rm opt}$ [see (5) and (6)]. Points are chosen with the same real or imaginary part as $\Gamma_{\rm opt}$, but with a maximized imaginary ($\Gamma = R_{\rm opt} + j \cdot X_{\rm max}$) and real ($\Gamma = R_{\rm max} + j \cdot X_{\rm opt}$) part, respectively [see Fig. 3(c)]. Of course, we still account for the maximum reflection coefficient achievable with the given setup.

The remaining two points are used to further optimize the pattern for the determination of $F_{\rm min}$ and R_n. Based on the qualitative conclusion for R_n and (7), we choose points around $\Gamma_{\rm opt}$ (for $F_{\rm min}$), but not too close to it (for R_n). We (more or less arbitrarily) selected the center of gravity of the triangles formed by the origin of the Smith chart, $\Gamma_{\rm opt}$, and two of the remaining four points of the original cross closest to $\Gamma_{\rm opt}$ [see Fig. 3(d)].

This selection procedure covers all criteria mentioned in Section IV-A and has the additional advantage of the reasonable simplicity with which the selection criteria can be expressed mathematically. Furthermore, it is suitable for implementation in our noise measurement setup (Focus Microwaves, Inc., P.Q. Canada), or any other impedance-tuning system

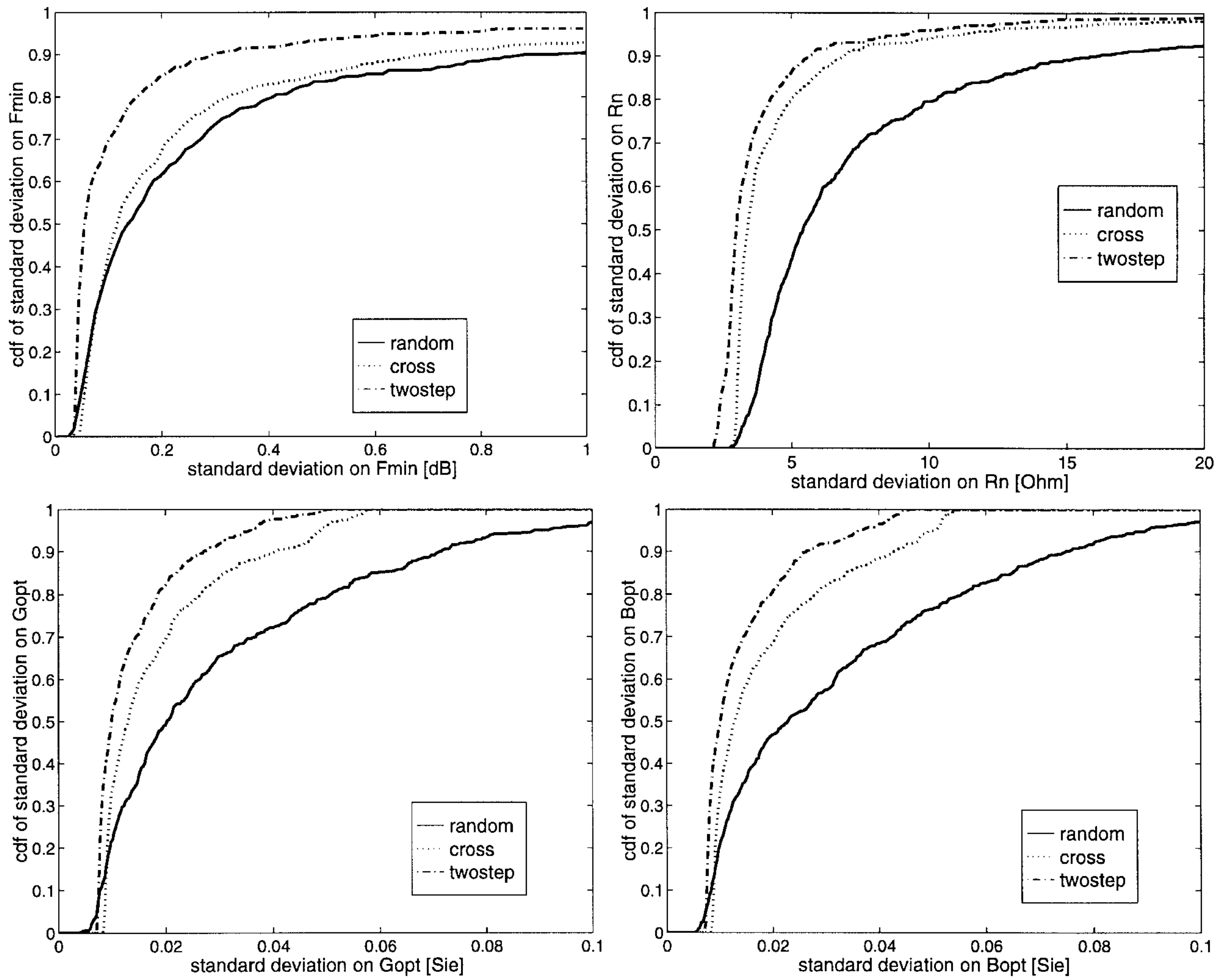

Fig. 4. Cumulative distribution for all four noise parameter's standard deviation and for random, cross, and two-step pattern. The position of Γ_{opt} was varied randomly.

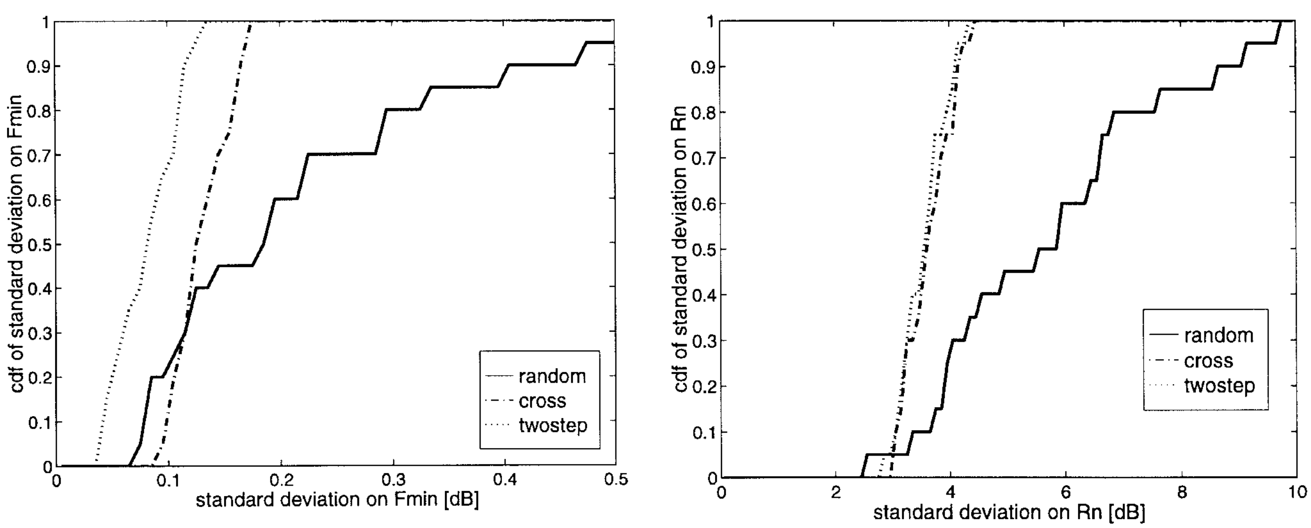

Fig. 5. Cumulative distribution for the standard deviation of $F_{\min}$ and R_n. $F_{\min}$ and R_n were varied on the left- and right-hand side, respectively.

offering a sufficiently dense coverage of the Smith chart. The tuner is characterized during calibration for each measurement frequency and a number of tuner positions. During measurement, interpolation between calibrated positions is possible.

With this method, we also performed the simulations described above. For each of the three methods we used, cumulative distribution functions (cdf's) were calculated for all four noise-parameter distributions, and for the variations of $F_{\min}$,

R_n, and Γ_{opt} described above. For a variation of Γ_{opt} (500 different locations) cdf's are shown for all four parameters in Fig. 4. For variations of $F_{\min}$ and R_n, they are shown only for $F_{\min}$ and R_n, respectively (see Fig. 5). In all circumstances, the new two-step method outperforms the cross-shaped and random pattern.

V. Conclusion

We investigated the relation between the admittance pattern for automatic noise-parameter determination and the accuracy on extracted parameters using a statistical approach. Our results indicate that the optimum pattern is different for each parameter. Based on numerous simulations of random patterns, we identified selection criteria for near-optimal patterns and verified them mathematically. We also proposed a new two-step pattern suitable for automatic pattern generation and showed that it outperforms random and cross-shaped patterns in a wide range of cases. These results are important for reliable extraction of noise parameters with an automatic measurement setup.

Acknowledgment

The authors wish to thank D. Dubouil and S, Bali, Focus Microwaves, P.Q., Canada, for their assistance with the tuner system.

References

[1] R. Q. Lane, "The determination of device noise parameters," *Proc. IEEE*, vol. 57, pp. 1461–1462, Aug. 1969.

[2] A. C. Davidson, B. W. Leake, and E. Strid, "Accuracy improvements in microwave noise parameter measurements," *IEEE Trans. Microwave Theory Tech.*, vol. 37, pp. 1973–1978, Dec. 1989.

[3] M. Sannino, "On the determination of device noise and gain parameters," *Proc IEEE*, vol. 67, pp. 1364–1366, Sept. 1979.

[4] G. Vasilescu, G. Alquie, and M. Krim, "Exact computation of two-port noise parameters," *Electron. Lett.*, vol. 25, pp. 292–293, Feb. 1989.

[5] M. Mitama and H. Katoh, "An improved computational method for noise parameter measurement," *IEEE Trans. Microwave Theory Tech.*, vol. MTT-27, pp. 612–615, June 1979.

[6] A. Boudiaf *et al.*, "Accuracy improvements in two-port noise parameter extraction method," in *IEEE MTT-S Int. Microwave Symp. Dig.*, Albuquerque, NM, 1992, pp. 1569–1572.

[7] L. Escotte, R. Plana, and J. Graffeuil, "Evaluation of noise parameter extraction methods," *IEEE Trans. Microwave Theory Tech.*, vol. 41, pp. 382–387, Mar. 1993.

[8] R. A. Pucel, H. A. Haus, and H. Statz, "Signal and noise properties of gallium arsenide microwave field effect transistors," in *Advances in Electronics and Electron Physics*, vol. 38, L. Marton, Ed. New York: Academic, 1975, pp. 195–265.

Sven Van den Bosch (S'92–M'95) was born in Merksem, Belgium, in 1972. He received the masters degree in electronic engineering from Gent University, Gent, Belgium, in 1995, and is currently working toward the Ph.D. degree.

His research is focused on nonlinear and noise characterization and modeling of active devices.

Luc Martens (M'92) was born in Gent, Belgium, on May 14, 1963. He received the M.Sc. degree in electrical engineering and the Ph.D. degree from the University of Gent, Gent, Belgium, in 1986 and 1990, respectively.

From 1986 to 1990, he was a Research Assistant in the Department of Information Technology (INTEC) University of Gent, during which time his scientific work was focused on the physical aspects of hyperthermic cancer therapy. His research dealt with electromagnetic and thermal modeling, and with the development of measurement systems for that application. Since 1991, he has been a Member of the permanent staff of the Interuniversity MicroElectronics Centre (IMEC), where he has been responsible for the research on characterization of packaging technologies with respect to high-frequency and electromagnetic compatibility (EMC) behavior and for the research on experimental modeling of active devices. He is also further studying topics related to the health effects of wireless communication devices. Since 1993, he has been a Professor of electrical applications of electromagnetism at the University of Gent.